View metadata, citation and similar papers at core.ac.uk

brought to you by CORE

provided by Elsevier - Publisher Connector

Arabian Journal of Chemistry (2015) **8**, 837–849

King Saud University

Arabian Journal of Chemistry

www.ksu.edu.sa
www.sciencedirect.com

ORIGINAL ARTICLE

Study of the adsorption of Cd (II) from aqueous solution using zeolite-based geopolymer, synthesized from coal fly ash; kinetic, isotherm and thermodynamic studies

Hamedreza Javadian [a], Forough Ghorbani [b], Habib-allah Tayebi [c,*], SeyedMostafa Hosseini Asl [d]

[a] *Young Researchers and Elite Club, Arak Branch, Islamic Azad University, Arak, Iran*
[b] *Department of Chemistry, Saveh Branch, Islamic Azad University, Saveh, Iran*
[c] *Department of Textile Engineering, Qaemshahr Branch, Islamic Azad University, Qaemshahr, Iran*
[d] *Department of Chemical Engineering, Shahrood Branch, Islamic Azad University, Shahrood, Iran*

Received 27 August 2012; accepted 27 February 2013
Available online 14 March 2013

KEYWORDS

Adsorption;
Cadmium;
Fly-ash;
Wastewater;
Kinetics

Abstract A specific type of zeolite, synthesized from coal fly ash, was used in our batch adsorption experiments in order to adsorb Cd (II) ions from aqueous solution. Solid-state conversion of fly ash to an amorphous aluminosilicate adsorbent (geopolymer) was investigated under specific conditions. The adsorbent ZFA was characterized using XRD, XRF, FT-IR, FE-SEM, LPS and BET surface area. The optimum conditions of sorption were found to be: a ZFA dose of 0.08 g in 25 mL of Cd (II) with contact time of 7 h and pH 5. Four equations, namely Morris–Weber, Lagergren, Pseudo-second order and Elovich have been used in order to determine the kinetics of removal process. The collected kinetic data showed that pseudo-second order equations controlled the adsorption process. According to adsorption isotherm studies, the Langmuir isotherm was proved to be the best fit for our experimental data, in comparison to Freundlich, D–R and Tempkin models. The thermodynamic parameters ΔH, ΔS and ΔG are evaluated. Thermodynamic parameters showed that the adsorption of Cd (II) onto ZFA was feasible, spontaneous and endothermic under studied conditions. To conduct desorption experiments, several solvents (including alkaline, bases and water) have been employed. 84% of desorption efficiency was achieved using NaOH.
© 2013 King Saud University. Production and hosting by Elsevier B.V. All rights reserved.

* Corresponding author.
E-mail address: tayebi_h@yahoo.com (H.-a. Tayebi).
Peer review under responsibility of King Saud University.

Production and hosting by Elsevier

1. Introduction

Nowadays, removing the toxic heavy metal contaminants from aqueous waste streams is one of the greatest matters of interest in the literature and studies. The main concern of environmentalists about heavy metals is that these elements are highly

1878-5352 © 2013 King Saud University. Production and hosting by Elsevier B.V. All rights reserved.
http://dx.doi.org/10.1016/j.arabjc.2013.02.018

toxic and their detrimental impact on human health and surroundings is grave (Aklil et al., 2004). Cadmium is one of the most toxic metals even in low concentrations. It is naturally produced in the environment and is a major contaminant. Cadmium (Cd) toxicity causes disorders such as heart disease, cancer and diabetes. Cadmium poisoning may also result in lung cancer, anemia, skin, pulmonary edema, bone diseases, brain damage and trachea-bronchitis (Voegelin and Kretzschmar, 2003; Tsang and Lo, 2006; Mohan et al., 2005; Deng and Ting, 2005). Cadmium accumulates in bone, liver and kidney and is even more poisonous than mercury. Taking in any considerable amount of Cd leads to instantaneous intoxication and damage to the liver and the kidney (Mohan et al., 2005; Deng and Ting, 2005). Cadmium is mainly formed when waste streams are discharged from metallurgical alloying, ceramics, metal plating and sewage sludge. Conventional methods including, reverse osmosis (Benito and Ruíz, 2002) electrodialysis (Mohammadi et al., 2005), ion-exchange (Dbrowski et al., 2004), chemical precipitation (Matlock et al., 2002), ultrafiltration (Ennigrou et al., 2009) and adsorption are used for removal of heavy metal ions from aqueous solutions. The adsorption method, among all above-mentioned processes, is the most preferable one because it is economically advantageous, highly efficient and applicable (Barrera-Díaz et al., 2005; Mohan and Pittman, 2006). Fly ash is a by-product of coal combustion occurring in various industrial processes. It is counted as an irritant which accounts for air pollution and also poses disposal difficulties. The fact that coal is used as a fuel in most industries causes fly ash to be produced in higher amounts, and this, in turn, causes many problems. The above-mentioned factors restrict the usage of fly ash in industries. The process of converting fly ash into crystalline zeolite or amorphous geopolymers has recently been a great matter of consideration. Due to its valuable properties such as ion exchange capability, natural and synthetic zeolite has gained a remarkable interest among researchers. The most prevalent method for converting fly ash into zeolite or geopolymer embraces a hydrothermal process, through which the fly ash is mixed with an alkali solution, like sodium hydroxide, under specific conditions. Recently, a new process has been proposed under the name of fusion method as it adds an alkaline fusion stage before the conventional zeolite synthesis process (Molina and Poole, 2004; Querol et al., 2002). In contrast, being a distinct group of quasi-ceramic materials, geopolymers are formed by a geosynthetic reaction of aluminosilicate minerals in the presence of an alkali solution at low temperatures (< 100 °C) (Davidovits, 1991; Xu and VanDeventer, 2000). Geopolymers are considered as the amorphous parallel for certain synthetic zeolites. Fly ash based geopolymers are pretty much reliant on cheap and readily available waste fly ash as the chief food supply, and thus, they enjoy a growing commercial potentiality. In recent few years, geopolymers have also been utilized for immobilizing and stabilizing pure or contaminated (mixed waste) forms of low-level radioactive waste and heavy metals as well (Phair et al., 2004; Van Jaarsveld et al., 1999). In recent studies, researchers have investigated the fusion method to see whether extracting aluminosilicate from fly ash and preparing mesoporous materials using supernatant is possible or not (Chang et al., 1999; Kumar et al., 2001).

They did not investigate the properties of the residual after extraction of fly ash, though. In this study, we have investigated the capability of the fusion solid-state reaction to convert fly ash at special conditions and also characterized the residual material as geopolymer-based absorbents and their usage in removing heavy metals from an aqueous solution. Hereby, we will compare the adsorption capacity of synthesized absorbents using raw fly ash and study the adsorption kinetics and isotherm for Cd (II) ions.

2. Materials and methods

2.1. Materials

Raw fly ash was procured from a combustion test furnace at the Alborz-e-sharghi Coal Company located in Shahrood, Iran. The ash was found to be friendly to the environment and its commercial applications are traced in traditional areas such as concrete production and building pavements and dams. Typical chemical composition of the ash is presented in Table 1. Standard solution of Cd (II) was prepared through the following process: First, cadmium nitrate [$Cd(NO_3)_2$] salt (Merck) was directly dissolved in 1000 mL of distilled water, then, the resultant solution was transferred to a 1-l volumetric flask and diluted to a volume determined in advance. The desired cadmium solutions were freshly prepared by diluting the stock solution using distilled water. All the chemicals employed in this study were of analytical grade (by Merck). For pH adjusting purpose, solutions of HCl (1 M, 0.1 M), HNO_3 (1 M, 0.1 M) and NaOH (1 M, 0.1 M) were prepared.

2.2. Adsorbent synthesis

In order to maintain a uniform particle size of 75 μm, fly ash was mechanically riddled using mechanical sieves. The fly ash was frequently rinsed with deionized water in order to remove the earthen impurities from it. The solids were dried at 100 °C and subsequently converted to powder. To produce ZFA, 6 g of fly ash was mixed with 7.2 g of solid NaOH and then the mixture was ground into fine powder (Brown). The powder, subsequently, was kept at 600 °C for 2 h, under a loose dark green lamp. The solids, after NaOH fusion treatment, were ground into powder and then, 60 mL of deionized water was added to it, and finally, it was heated to 95 °C for about 75 h by magnetic stirring at 400 rpm. The suspension took the form of a dark green supernatant lying over brown solid residues. The slurry was then secured in a Teflon-lined autoclave and kept at 140 °C for 72 h. The resulting sample was finally filtered, washed for several cycles with deionized water until it became neutral (pH < 7) and dried at 100 °C. The ZFA color turned dark brown and was utilized in further sorption experiments.

Table 1 Chemical composition of fly ash in this study by XRF.

Properties	LIO	SiO_2	Al_2O_3	Fe_2O_3	CaO	MgO	SO_3	K_2O	Na_2O
Percentage (wt.%)	0.98	37.88	28.73	18.07	11.54	1.79	0.38	0.34	0.29

2.3. Analysis

The X-ray diffraction (XRD) patterns of ZFA and RFA were prepared using a X-ray diffractometer (GBC made, Australia). The operating conditions were 35 kV and 28.5 mA. Cu and K_α were used as radioactive sources. Samples were scanned in the range of 10–0°, and JCPDS (Joint Committee on Powder Diffraction Standards) files were utilized in identifying the crystalline compounds. The surface morphology of RFA and ZFA was observed using a Field Emission Scanning Electron Microscope (FE-SEM) (HITACHI, S-4160, Japan).

The functional groups of RFA and ZFA were tested using Fourier transform infrared spectrometry (FT-IR) (ECTOR-UKER, Germany) in the region of 4000–400 cm^{-1} wavenumbers. A laser particle sizer (Master size 2000, Malvern Co., UK) was employed to analyze the particle size distribution of the two samples. We have determined the BET (Brunauer–Emmet–Teller) specific surface area by fitting the linear portion of BET plot to BET equation; based upon the desorption plot of N_2 adsorption–desorption isotherm and using the Barret-Joyner-Halenda (BJH) method (Micrometrics ASAP 2000, USA), pore size distribution was calculated. Using the water displacement method, Skeleton density and porosity of ZFA and RFA were measured. In addition to the above-mentioned method, the following equation was also used to calculate the value of porosity (Lin and Wu, 2001):

$$\varepsilon_p = 1 - \rho_s/\rho_p \quad (1)$$

where ε_p is the porosity of adsorbent, ρ_s, the skeleton density of adsorbent (g cm^{-3}) and ρ_p. The density of RFA (g cm^{-3}). After the occurrence of adsorption reaction, the supernatants were gathered and Cd (II) concentration has been measured using an atomic absorption spectrophotometer (Model GBC 302, Australia).

2.4. Batch sorption tests

Several adsorption experiments were carried out in this study in order to investigate the effect of experimental conditions on achieving the highest amount of cadmium removal. To optimize the process of removing Cd (II), different parameters such as, the effects of rotating speed, pH, contact time, dosage of the adsorbent and the initial concentration of Cd (II) has been taken into consideration. Isotherm kinetics were also evaluated in this part of the study. The pH of the solution was adjusted either by a pH-meter or also using HNO_3 and NaOH solutions. In each stage, equal amounts of adsorbent were added to the samples, and then, the solutions were mixed at an optimum rotating speed in a magnetic mixer. At the end of each predetermined time interval, the sorbent was filtered and the concentration of Cd (II) was determined. All experiments were carried out two times and the resultant adsorbed concentrations were used for duplicate experimental results. All the experiments were repeated twice, and the experimental error was below 4%. The average data were reported. In all of the experiments, ZFA was in the form of powder. The efficiency of Cd (II), % Removal, was calculated using:

$$\text{Removal efficiency}(\%) = (C_i - C_t)/C_i \times 100 \quad (2)$$

where C_i is the initial concentration (mg L^{-1}) and C_t, the concentration (mg L^{-1}) at any time t. The q value shows the amount of metal adsorbed per specific amount of adsorbent (mg g^{-1}). The sorption capacity at time t, q_t (mg g^{-1}), was obtained as follows:

$$q_t = (C_i - C_t) \times V/M \quad (3)$$

where C_i and C_t (mg $/L^{-1}$) were the liquid-phase concentrations of solutes at initial and a given time t, V is the volume of the solution and M, the mass of ZFA (g). The amount of adsorption at equilibrium, q_e, was calculated using:

$$q_e = (C_i - C_e) \times V/M \quad (4)$$

where C_e (mg L^{-1}) was the ion concentration at equilibrium.

2.5. Desorption experiments

As previously mentioned in the adsorption process, the adsorbent was dispersed in 50 mg L^{-1} of Cd (II) solution. The Cd (II)-loaded adsorbent was separated from the mixture solution through the centrifugation process and then washed with distilled water to remove any unabsorbed metal ions. Desorption experiment was conducted by transferring the Cd (II)-loaded ZFA into 50 mL of distilled water, HCl, HNO_3 and NaOH. Then the solution was stirred for 24 h. The adsorbent, after being regenerated, was utilized once more for further adsorption of Cd (II). Adsorption and desorption experiments were repeated for three cycles.

3. Results and discussion

3.1. Characterization of the adsorbents

The X-ray diffraction (XRD) patterns of RFA and ZFA are demonstrated in Fig. 1. The main diffraction peaks of RFA are attributed to quartz (SiO_2), hematite (Fe_2O_3), anhydrite ($CaSO_4$), magnetite (Fe_3O_4) and lime (CaO). In contrast to the previous report, aluminum mineralogical phases, such as mullite, despite the existence of 28.73% Al_2O_3 in the raw fly ash, could not be found in the material (Table 1). In the XRD pattern of RFA, the quartz becomes the main crystalline phase and minor hematite, magnetite and anhydrite still exist. This indicates that the content of quartz increases and the mineral containing elemental Fe (hematite and magnetite) decreases after the fusion treatment process is done. Unlike RFA, no new diffraction peak appears and no new crystalline phase is observed in the XRD pattern of ZFA. Even the diffraction peaks of magnetite disappear, showing that the created new substance on the surface of the ZFA is amorphous. Most crystalline phases disappeared for the treated fly ash, and an amorphous phase occurred, which corresponds to geopolymer.

Fig. 2 illustrates the FT-IR transmittance spectra of RFA and ZFA. Unlike RFA, the adsorption at 1135 cm^{-1} is assigned to the vibration of Fe–O bond, and the band at 1033 cm^{-1} is assigned to the asymmetric stretching vibration of T–O (T=Si, Al) bonds (Fan et al., 2008). Typical bonds of quartz become clearer; this can be due to the inactivity of quart and the resultant enrichment in the ZFA (El-Naggar et al., 2008). The new bonds in the spectra of ZFA and RFA, at 3573 and 3421 cm^{-1}, are assigned to O–H vibration, which respectively correspond the two O–H stretching vibration and to deformation vibration bond; this suggests that the new substance loaded in the ZFA exists in the form of

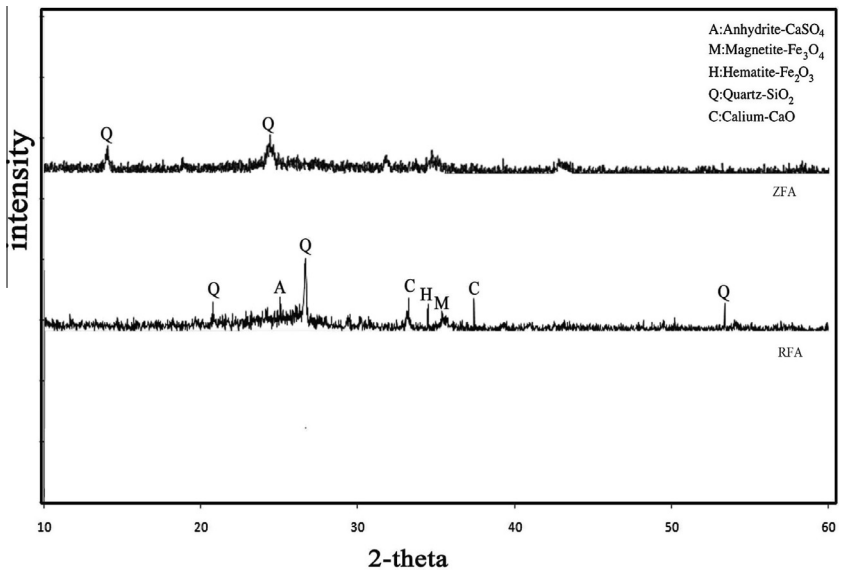

Figure 1 X-ray diffraction patterns of RFA and ZFA.

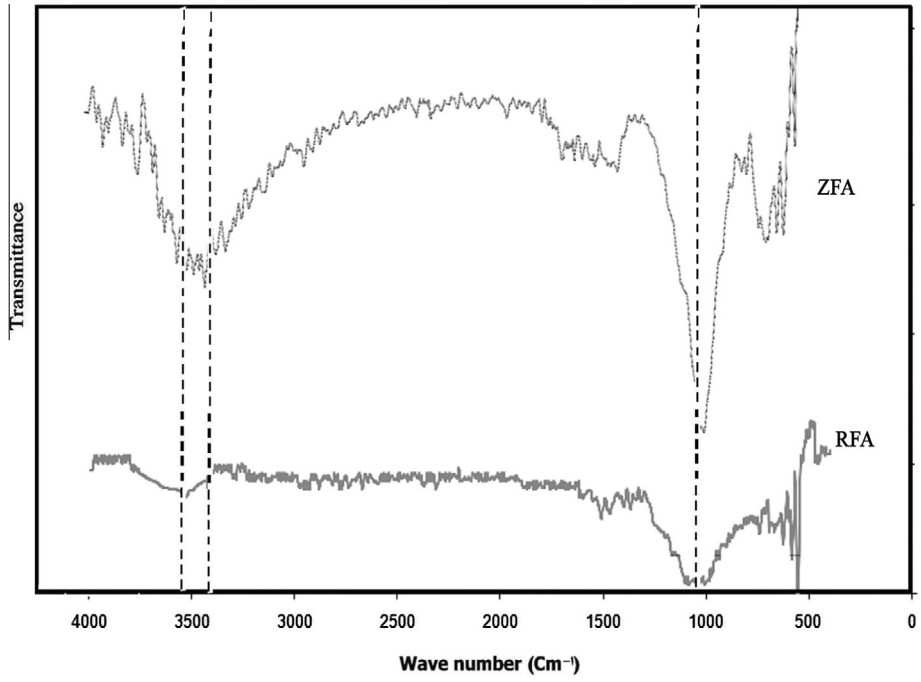

Figure 2 FT-IR spectra of RFA and ZFA.

hydroxyl compound (Gonźalez et al., 2001). According to the FT-IR of RFA and ZFA, a strong broad band exists at 3511 and 3421 cm^{-1} which evidences the presence of hydroxyl groups on the fly ash (Boonamnuayvitaya et al., 2004). A sharp peak is observed at 1033 and 1010 cm^{-1} for RFA and ZFA which may be formed due to the presence of Al atoms in the tetrahedral forms of silica frame work (Shoval, 2003). The band which exists at 734 and 622 cm^{-1} for RFA and 723 and 692 cm^{-1} for ZFA corresponds to the existing quartz in the fly ash (Jimenez and Palomo, 2005). The band emerging between 800 and 500 cm^{-1} is pertinent to the tetrahedral vibrations, formed by what we recognize as the secondary building units (SBU) and fragments of the alumina silicate system. These bands represent the typical features of double or single rings (depending on the structure of the material) and or the TO_4 (T=Si, Al) tetrahedral bonds (Mohan and Gandhimathi, 2009).

The changes in the morphology of RFA and ZFA are depicted in Fig. 3a and b. These images show that the final powder is dramatically different from the original ash. The surface of ZFA is entirely coated with the hydroxyl compounds and penetrates the porous network structure, whereas the size of granule also increases sharply. According to the data obtained from analysis, the mean particle size of RFA and ZFA is 4.18 and 17.21 μm, respectively. The end-product is nearly four

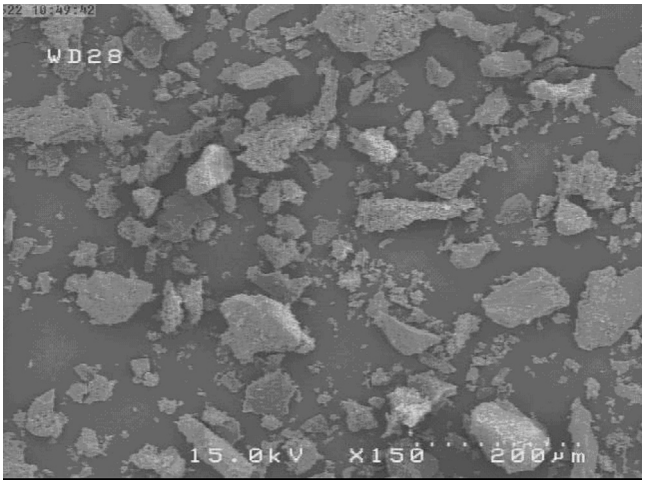

Figure 3a FE-SEM images of RFA.

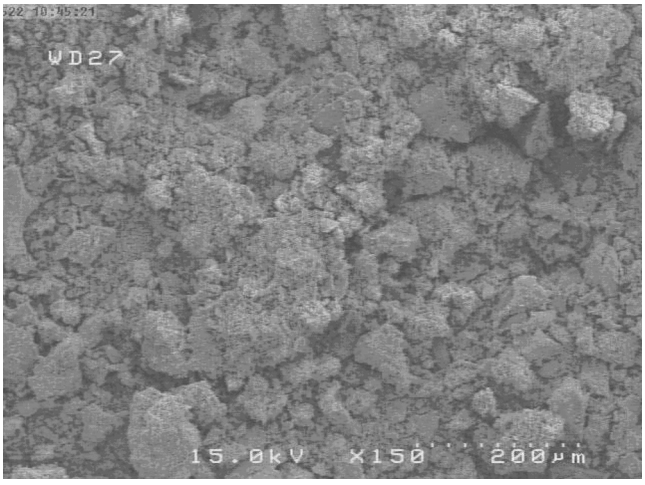

Figure 3b FE-SEM images of ZFA.

times as large as RFA, which can effectively improve the separation effect after adsorption treatment. In a blank test done for comparison, an equivalent RFA was replaced with ZFA in order to remove Cd (II) from the solution under same conditions. The different types of sorption evidence the existence of the mesoporous structure in the material. Regarding the pore size distribution, it is understood that the pore size of ZFA ranged from 18 Å to 530 Å, the average pore size was 29 Å, and porosity was 19.82%.

3.2. Effect of pH

The initial pH range of 2–12 was used to study the effect of pH of the solution on removing Cd (II) by ZFA. Fig. 4 illustrates the effective removal of Cd (II) in the initial pH range of 2–5. The efficiency of Cd (II) removal decreased as the pH was raised. The amount of Cd (II) removed in pH of 5, was found to be 14.431 mg g^{-1}. This way, it is understood that ZFA was effective over a wider range of pH than other adsorbents. The potentiality of ZFA to be used in a wide pH range could be due to the aluminum hydroxide present on the surface of the adsorbents, as it is effective in a wide range on Cd (II) removal.

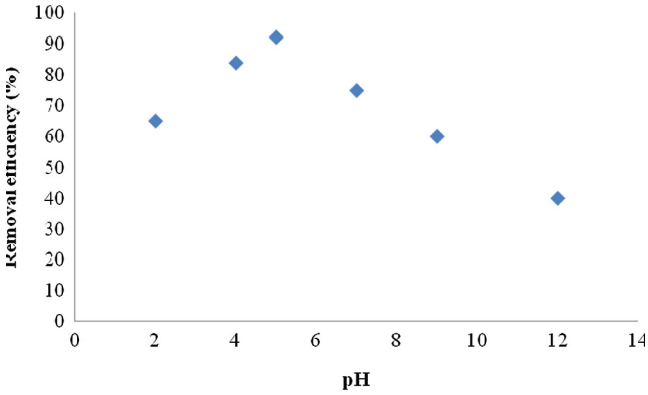

Figure 4 The effect of pH on the removal efficiency.

Consequently, the removal mechanisms of ZFA for the Cd (II) include not only adsorption but also reaction with the oxide of both iron and aluminum on the surface of ZFA (Langmuir, 1916). To compare the removal amounts of Cd (II) by ZFA and the raw fly ash, the test was carried out at pH = 5 under similar conditions. The amounts of removal obtained using raw ash and ZFA were respectively 7 and 14.431 mg g^{-1} which indicated that ZFA was much more effective than the raw ash and its capability in removing Cd (II) was two times as high as that of the raw fly ash under the same condition. This phenomenon could chiefly be ascribed to the porous structure on the surface of ZFA; hereby, the high surface area, e.g. the BET surface area, for ZFA and RFA was 8.22 and 130.45 m^2 g^{-1}, respectively. When hydroxyl compounds were loaded on the surface of residual fly ash, the specific surface area was consequently increased nearly 15 times in comparison to fly ash; therefore, the efficiency of adsorption was greatly improved.

3.3. Effect of contact time

Kinetic adsorption experiments were done in order to calculate the adsorption equilibrium time. In these experiments, the dosage of ZFA was 0.08 g L^{-1} and the initial cadmium concentration was 50 mg L^{-1}. The data pertinent to contact time and Cd (II) removal amount by the ZFA are given in Fig. 5. The results indicated that Cd (II) removal occurred in the first 5 h and the adsorption equilibrium was achieved in 7 h.

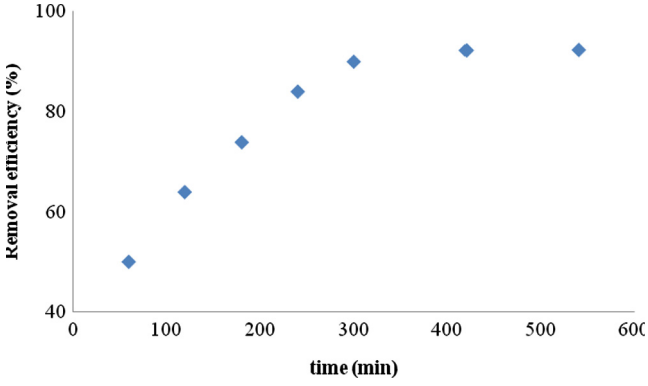

Figure 5 The effect of contact time on the removal efficiency.

3.4. Effect of adsorbent dosage

Fig. 6 shows the effect of adsorbent dosage on Cd (II) removal. With an increase in the dosage of adsorbent, the removal efficiency of Cd (II) sharply increased. From this point on, as more dosages of adsorbent were added to the solution, the increase in the removal amount advanced slowly and when more adsorbents were added to the solution, cadmium became fully adsorbed.

3.5. Effect of initial concentration of Cd (II)

Cadmium solutions of various initial concentrations from 10 mg L^{-1} to 100 mg L^{-1} were treated with 0.08 g of adsorbent at pH = 5. The effect of varying concentration of Cd (II) on the removal efficiency of the cadmium is shown in Fig. 7. As it was already expected, the removal efficiency of Cd (II) declined as the initial Cd (II) concentration increased. This demonstrated that the amount of Cd (II) adsorption by the ZFA is dependent upon the availability of binding sites for cadmium. The removal efficiency of Cd (II) could reach above 96% only when the primary concentration of Cd (II) was 10 mg L^{-1}.

3.6. Kinetics of sorption

Various kinetic models, including Morris–Weber, Lagergren, Pseudo-second order and Elovich models have been utilized due to their consistency with the experimental adsorption data, obtained for adsorption of Cd (II) onto ZFA. No mass transfer (either external or internal) resistance was expected to happen to the overall adsorption process. Therefore kinetics can be studied based upon the concentration of residual metal ion in the solution. Studying kinetics of adsorption helps us to find out the solute uptake rates which, clearly, can be used to control the residence time of adsorbate uptake at solid-solution interface including the diffusion process.

3.6.1. Morris–Weber kinetic model

In order to investigate the changes that occurred in the concentration of sorbate onto sorbent with shaking time, the kinetic data of Cd (II) ions sorption onto ZFA were fitted into (Morris and Weber, 1963):

$$q_t = K_{id}(t)^{0.5} + C \quad (5)$$

where q_t is the sorbed concentration of Cd (II) ions at time 't'. The plot of q_t vs. $t^{0.5}$ is given in Fig. 8. The value of rate constant of Morris–Weber transport, K_{id}, is calculated using the slope of the linear plot. The rate constant K_{id} = 0.445 h^{-1} was calculated from the slope of the straight line with a correlation factor of 0.8855.

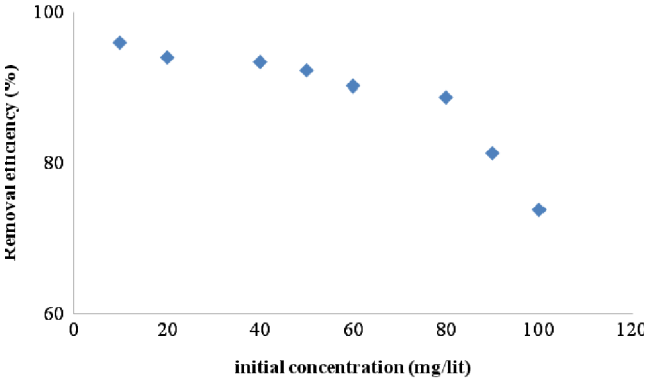

Figure 7 The effect of initial concentration on the removal efficiency.

Internal particle diffusion may encompass pore and/or surface diffusion. The intra-particle diffusion plots bespoke of multi-linearity in the process showing that there exist three operational steps. The first stage is the diffusion of adsorbate through the solution on the external surface of the adsorbent or the boundary surface diffusion of the sorbate molecules. The second stage precisely shows the gradual sorption, where intra-particle diffusion is rate-limiting, and the third stage is related to the final equilibrium achieved due to the extremely low sorbate concentration left in solution and reduction of interior active sites. The three stages in the plot propose that the sorption process occurs through surface adsorption and intra-particle diffusion.

3.6.2. Lagergren kinetic model

In 1898 (Lagergren, 1898), Lagergren, based on solid capacity, suggested a pseudo-first-order equation for the sorption of liquid/solid system. This system declares that the rate of change that occurred in sorbate uptake with the passage of time is directly proportional to the difference in the saturation concentration and the rate of solid uptake with time. The Lagergren equation is the most commonly used rate equation in liquid phase sorption. The general equation is brought as:

$$\ln(q_e - q_t) = \ln q_e - Kt \quad (6)$$

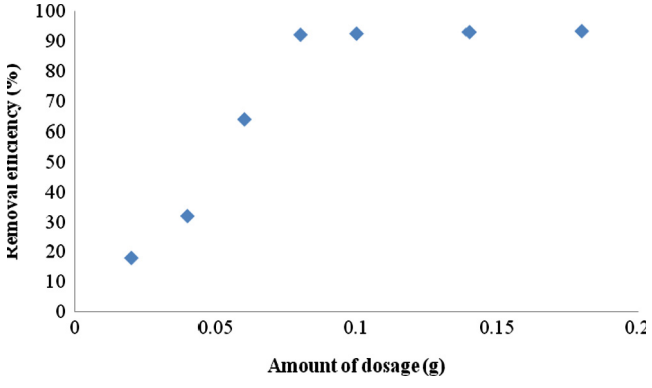

Figure 6 The effect of amount of ZFA on the removal efficiency.

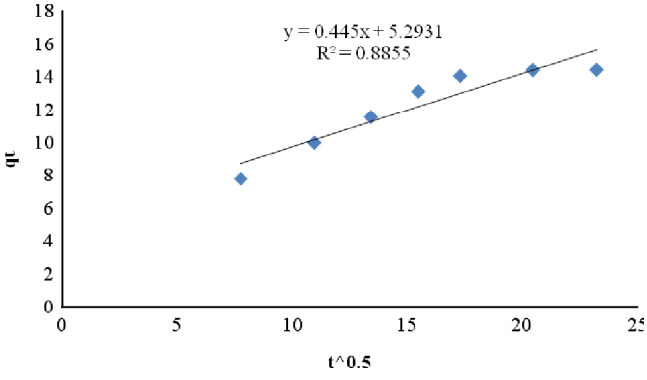

Figure 8 Morris–Weber plot of Cd (II) ions sorption onto ZFA.

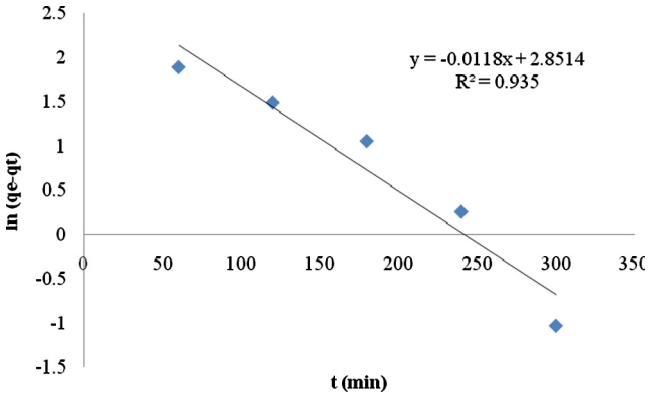

Figure 9 Validation of Lagergren plot of Cd (II) ions sorption onto ZFA.

where q_e is the sorbed concentration at equilibrium and K, the first order rate constant. The linear plot of ln ($q_e - q_t$) against time 't' (Fig. 9) depicts the applicability of the above-mentioned equation for sorption of Cd (II) ions onto ZFA. The rate constant $K = 0.0118\ h^{-1}$ was calculated from the slope of the straight line with a correlation factor of 0.935. The obtained kinetic data proved that the adsorption process was controlled by the pseudo first-order equation.

3.6.3. Pseudo-second order kinetic model

The sorption of Cd (II) ions onto ZFA following pseudo-second-order kinetics can be represented as (Ho and McKay, 1999):

$$q_t = k_2 q_e^2 t/1 + k_2 q_e t \quad (7)$$

where q_t and q_e are the amount of ion adsorbed at time t and at equilibrium (mg g^{-1}) and k_2(g mg^{-1} min^{-1}) is the pseudo-second-order rate constant for the adsorption process.

This equation can be linearized to four different forms. The different linearized types of the pseudo second-order equation are given in Table 2. From the results, adsorption of Cd (II) by ZFA can be made fit using Type 1, Type 2, Type 3, and Type 4 equations; Also Type1 equation offers a best correlation factor.

Fig. 10a–d show the linear plot of different Type of pseudo second-order equation. The rate constant was calculated from the slope of the straight line. The rate constant $K_2 = 0.000869\ h^{-1}$ was calculated from the slope of the straight line with a correlation factor of 0.9964 (Fig. 10a). This implies the assumption of pseudo-second-order model saying that the process of Cd (II) uptake is due to chemisorptions (Hui et al., 2005). According to this assumption, chemisorption's involving valence forces act as the rate-limiting step by making the adsorbent and adsorbate to exchange electrons. It is worth to note that the mechanism, with which an adsorbent adsorbs multi-metal ions, is very complicated. Factors affecting the behavior of each metal ion in a system of multi-metal ions include the concentration and the properties of other present ions, pH of the solution, physical and chemical properties of both the adsorbent and the adsorbate. The shape and adsorption kinetics of the system were influenced by both interaction and competition effects between multi-metal ions (Ho and McKay, 2000).

3.6.4. Elovich kinetic model

Elovich equation is given as (Gerente et al., 2007):

$$q_t = 1/\beta \ln(\alpha\beta) + 1/\beta \ln t \quad (8)$$

where α (mmol g^{-1} min^{-1}) is the initial adsorption rate and β (g $mmol^{-1}$) is the desorption constant related to the extent of surface coverage and activation energy for chemisorption. The slope and the intercept of the plot of q_t vs. ln t (Fig. 11) result in the determination of the kinetic constants α and β. The rate constants were $\alpha = 0.623$ and $\beta = 0.3037$ with a correlation factor of 0.9571.

The obtained statistical data and kinetic constants are presented in Table 2. For Cd (II) adsorption, the obtained kinetic data proved that the adsorption process was controlled by the Pseudo second-order model.

3.7. The isotherm model

The adsorption isotherm model is based upon the hypothesis saying that all adsorption sites are equivalent and their status does not depend on whether the neighboring sites are occupied or not. Isotherms describe the relationship between the metal content of a solution and the amount of metal adsorbed on a specific adsorbent at a constant temperature.

3.7.1. The Langmuir isotherm model

The Langmuir model is valid and applicable to adsorptions onto a surface containing a limited number of identical

Table 2 Kinetic constants for Cd (II) adsorption.

Lagergren	K (min^{-1})	)q_e) mg/g	R^2
	0.0118	17.312	0.935
Pseudo-second order	k_2(g mg^{-1} min)	)q_e) mg g^{-1}	R^2
Type 1 $t/q_t = 1/(k_2 q_e^2) + (1/q_e)t$ t/q_t vs. t	0.000869	16.583	0.9964
Type 2 $1/q_t = 1/q_e + 1/k_2 q_e^2$ $(1/t)$ $1/q_t$ vs. $1/t$	0.000873	16.528	0.9826
Type 3 $q_t = q_e - 1/k_2 q_e(q_t/t)$ q_t vs. q_t/t	0.000849	16.648	0.9535
Type 4 $q_t/t = k_2 q_e^2 - k_2 q_{e(}q_t)$ q_t/t vs. q_t	0.000801	16.851	0.9535
Morris–Weber	K_{id} (min^{-1})		R^2
	0.445		0.8855
Elovich	α	β	R^2
	0.623	0.3037	0.9571

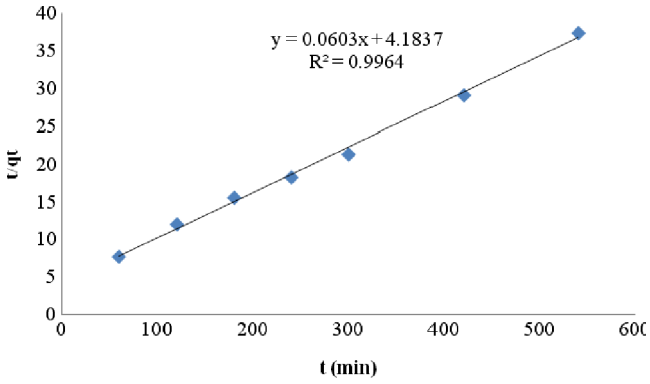

Figure 10a Pseudo second order (Type 1) plot of Cd (II) ions sorption onto ZFA.

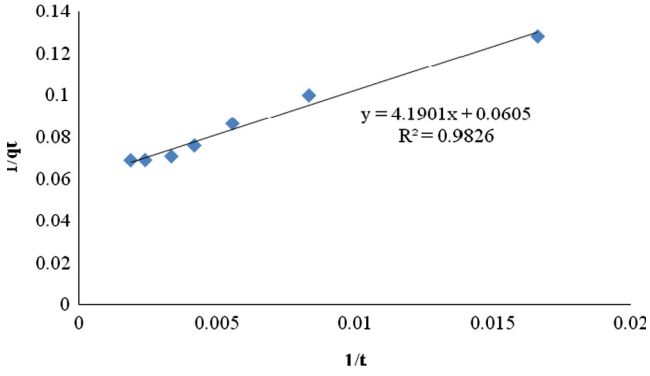

Figure 10b Pseudo second order (Type 2) plot of Cd (II) ions sorption onto ZFA.

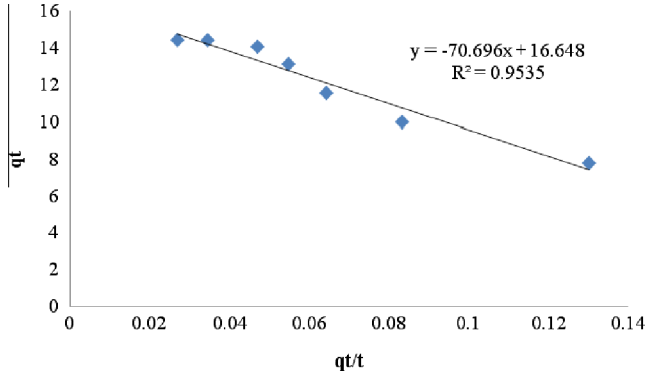

Figure 10c Pseudo second order (Type 3) plot of Cd (II) ions sorption onto ZFA.

sorption sites. This isotherm is often offered in the form of the following equation (Langmuir, 1916):

$$q_e = q_m K_L C_e/(1 + K_L C_e) \quad (9)$$

where q_e is the amount of metal adsorbed per specific amount of adsorbent (mg g^{-1}), C_e, the equilibrium concentration of the solution (mg L^{-1}), and q_m, the maximum amount of adsorption metal ions (mg g^{-1}). We can remodel and rearrange this equation into four different linear types presented below in order to make plotting and determination of Langmuir constants

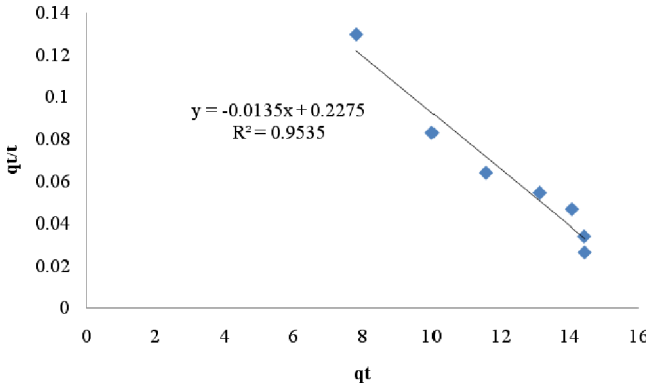

Figure 10d Pseudo second order (Type 4) plot of Cd (II) ions sorption onto ZFA.

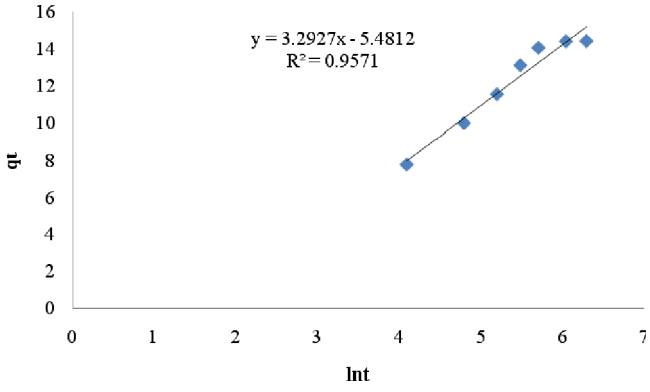

Figure 11 Elovich plot of Cd (II) ions sorption onto ZFA.

(K_L) and sorption capacity (q_m) from the slope easier Fig. 12a–d. The best fit was obtained by Langmuir Type 1 as compared with the other Langmuir models (Fig. 12a).

The fundamental characteristics and practicability of Langmuir isotherm regarding a dimensionless constant separation factor or equilibrium parameter R_L, are defined as (Weber and Chakraborti, 1974):

$$R_L = 1/1 + K_L C_i \quad (10)$$

where K_L is the Langmuir constant and C_i is the initial concentration of Cd (II). The R_L value depicts the shape of the isotherm (Table 3).

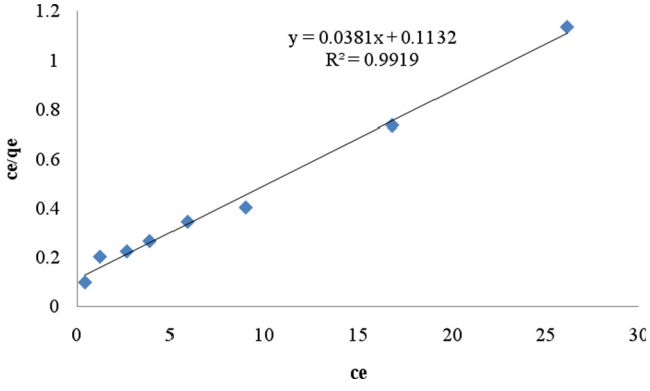

Figure 12a Langmuir sorption isotherm (Type 1) of Cd (II) ions onto ZFA.

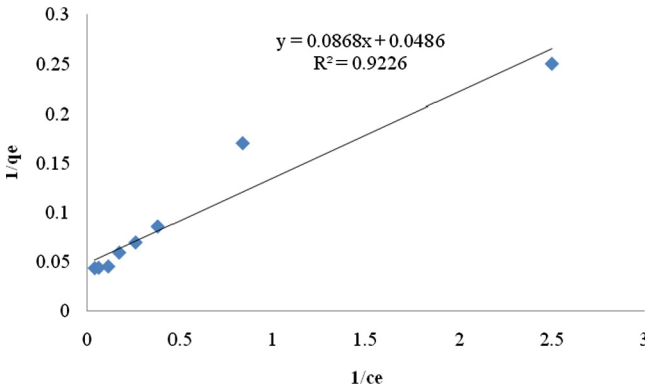

Figure 12b Langmuir sorption isotherm (Type 2) of Cd (II) ions onto ZFA.

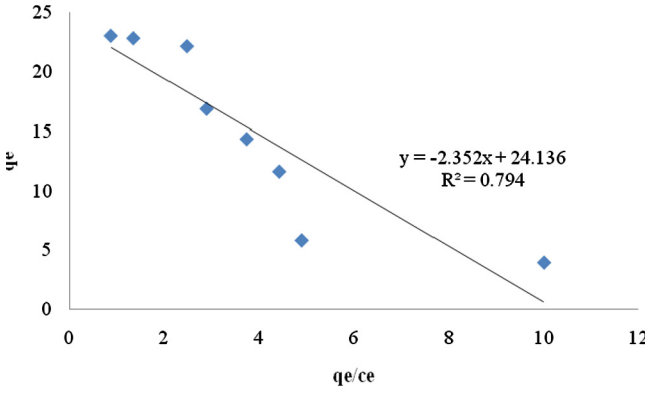

Figure 12c Langmuir sorption isotherm (Type 3) of Cd (II) ions onto ZFA.

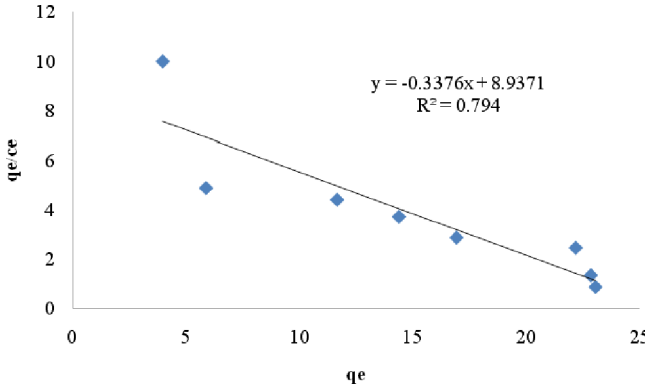

Figure 12d Langmuir sorption isotherm (Type 4) of Cd (II) ions onto ZFA.

Favorable amount of adsorption can be reached with a R_L between 0 and 1 (McKay et al., 1982). For concentration of 10–100 mg L^{-1} of Cd (II), the results are given in Table 4.

3.7.2. The Freundlich isotherm model

Unlike Langmuir isotherm, suggesting that enthalpy of adsorption is independent of the amount adsorbed, an experimental and data-based Freundlich equation can be attained based on sorption on heterogeneous surface which assumes a logarithmic decline in the enthalpy of adsorption as the fraction of occupied sites increases. The Freundlich equation is strictly empirical and based upon sorption on heterogeneous surface. The equation is presented as follows in the form of (Freundlich, 1906):

Table 3 Description of types of isotherm by R_L.

R_L Value	Types of isotherm
$R_L > 1$	Unfavorable
$R_L = 1$	Linear
$0 < R_L < 1$	Favorable
$R_L = 0$	Irreversible

$$q_e = K_F\,(C_e)^{1/n} \tag{11}$$

where K_F and $(1/n)$ are the Freundlich constant and the adsorption intensity, respectively. From the intercept and the slope of the linear plot of log q_e against log C_e, equilibrium constants can be determined based on experimental data. The Freundlich equation can be linearized in logarithmic form as Eq. (12) for the determination of the Freundlich constants:

$$\log\,(q_e) = \log\,(K_F) + (1/n)\log\,(C_e) \tag{12}$$

The slope and the intercept correspond to $(1/n)$ and K_F, respectively. It was revealed that the plot of log q_e and log C_e yields a straight line (Fig. 13).

3.7.3. The Tempkin isotherm model

This isotherm model involves a factor that fully allows for including the interactions between adsorbents and adsorbates. The Tempkin model accepts the following conditions: (i) the adsorption heat of all molecules present in the layer linearly decreases with the coverage which is because of adsorbent–adsorbate interactions; (ii) a uniform distribution of binding energies, up to maximum binding energy, is used to characterize the adsorption. The Tempkin isotherm proposes that the decrease in the heat of adsorption is more linear rather than logarithmic as already suggested implicitly by the Freundlich equation. The Tempkin isotherm is commonly used in the form of the following equation (Tempkin and Pyzhev, 1940):

$$q_e = B\ln\,(K_T\,C_e) \tag{13}$$

where $B = (RT/A_T)$ and K_T is Tempkin constant.

To simplify plotting and calculation of Tempkin constant, the above equation is often rearranged as the linear form offered below. The values of K_R and α_R can be calculated from the linear plot of q_e vs. ln (C_e) (Fig. 14).

$$q_e = B\ln\,K_T + B\ln\,C_e \tag{14}$$

The linearized form of the Tempkin adsorption isotherm presented in Eq. (16) was used to analyze the equilibrium data.

3.7.4. The Dubinin–Radushkevick isotherm model

The Dubinin–Radushkevick (D–R) (Dubilin and Radushkevich, 1947; Naiya et al., 2009; Ghazy and Ragab, 2007) isotherm was employed to specify the nature of the adsorption process through physisorption or chemisorption. The linear form of this model is described as:

$$\ln\,q_e = \ln\,q_m - \beta\,\varepsilon^2 \tag{15}$$

where q_e is the amount of adsorbed cadmium per unit dosage of the adsorbent (mg g^{-1}), q_m, the adsorption capacity, β, the

Table 4 Isotherm constants for Cd (II) adsorption.

Langmuir equation	K_L (mg L^{-1})	$)q_m)$mg g^{-1}	R_L	R^2
Type 1 $C_e/q_e = K_L/q_m + (1/q_m)C_e$ C_e/q_e vs. C_e	2.971	26.246	0.032–0.0033	0.9919
Type 2 $1/q_e = K_L/q_mC_e + 1/q_m$ $1/q_e$ vs. $1/C_e$	1.786	20.576	0.053–0.0055	0.9226
Type 3 $q_e = q_m - (K_L)$ q_e/C_e q_e vs. q_e/C_e	2.352	24.136	0.041–0.0042	0.794
Type 4 $q_e/C_e = q_m/K_L - q_e/K_L$ q_e/C_e vs. q_e	2.472	26.472	0.038–0.0040	0.794
Freundlich	K (L/g)	n		R^2
	6.603	2.164		0.9309
D–R	β	$)q_m)$ mg g^{-1}		R^2
	2×10^{-7}	17.059		0.7231
Tempkin	K_T	B		R^2
	0.0134	5.3195		0.9446

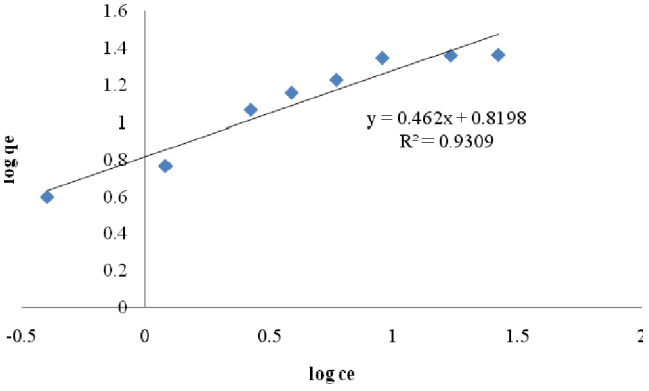

Figure 13 Freundlich sorption isotherm of Cd (II) ions onto ZF.

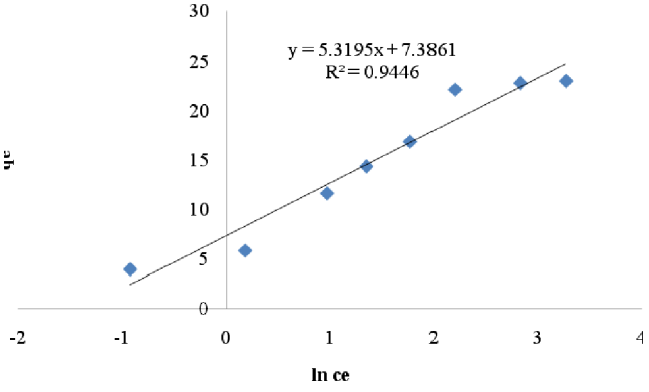

Figure 14 Tempkin sorption isotherm of Cd (II) ions onto ZFA.

activity coefficient pertinent to mean sorption energy and ε, the Polanyi potential, which can be calculated through Eq. (16):

$$\varepsilon = RT\ln\left[(1 + 1/C_e)\right] \quad (16)$$

Determination of the mean energy of sorption, E (kJ/mol), is done using the following equation Eq. (17):

$$E = 1/\sqrt{2\beta} \quad (17)$$

Hereby, the mean adsorption energy was found to be 1.581 kJ mol^{-1}.

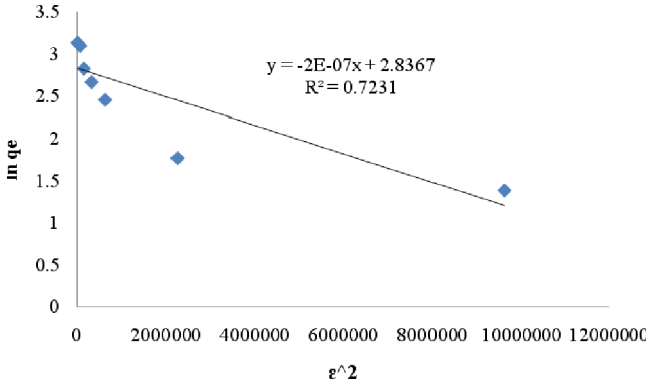

Figure 15 D–R sorption isotherm of Cd (II) ions onto ZFA.

This amount (E), obtained from the D–R model, is useful for it provides us with information about the mechanisms of adsorption process. If E value is between 8 and 16 kJ mol^{-1}, the type of adsorption process is chemical; however, if $E < 8$ kJ mol^{-1}, the process occurs physically.

The slope and the intercept of the linear plots of ln q_e vs. ε^2 (Fig. 15) were used to determine the values of β and q_m. The statistical results and also the isotherm constants are offered in Table 4. As it can be inferred from the results, adsorption of Cd (II) by ZFA can be made fit using Freundlich and Tempkin equations; Besides, Langmuir equation also offers a remarkable correlation factor. Freundlich isotherm, despite being able to provide us with information on surface heterogeneity and exponential distribution of the active sites and their energies, it cannot anticipate any saturation of the adsorbent surface by the adsorbate. Consequently, prediction of infinite surface coating can only be done mathematically. In contrast, D–R isotherm pertains to the heterogeneity of energies close to the adsorbent surface.

If we chose a very small sub-region of the sorption surface and consider it to be approximated by the Langmuir isotherm, the quantity can be pertained to the mean sorption energy, E, which stands for the free energy needed to transfer 1 mol of metal ions from infinity to the surface of the adsorbent (Naiya et al., 2008).

Table 5 The effect of temperature on removal efficiency.

Temperature °C	Removal efficiency (%)
25	92.28
35	94.16
45	97.45

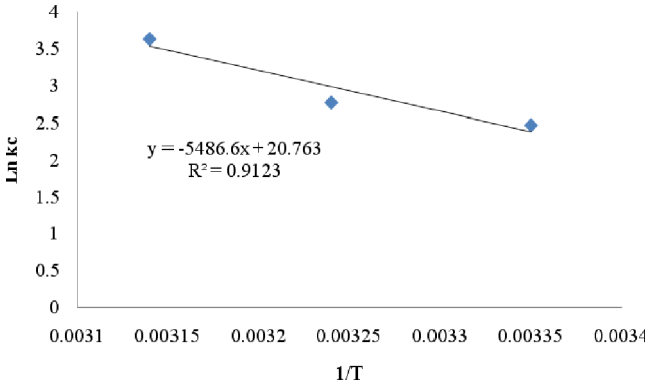

Figure 16 Ln K_C vs. $1/T$ for enthalpy and entropy change of the sorption process.

3.8. Thermodynamic study

3.8.1. Effect of temperature on adsorption of Cd (II)

To study the effect of temperature adsorption experiments are carried out at 25–45 °C at an optimum pH value of materials and an adsorbent dosage level of 0.08 g in 25 ml of solutions. The equilibrium contact time for adsorption was maintained at 7 h. The percentage of adsorption increases with the rise of temperature from 25 to 45 °C. The results were shown in Table 5 and it revealed the endothermic nature of the adsorption process which was later utilized for the determination of changes in Gibbs free energy (ΔG), heat of adsorption (ΔH) and entropy (ΔS) of the adsorption of Cd (II) from aqueous solutions. The increase in adsorption with rise in temperature may be due to the strengthening of adsorptive forces between the active sites of the adsorbents and adsorbate species and between the adjacent molecules of the adsorbed phase (Kumar et al., 2008).

3.8.2. Effect of temperature on thermodynamics parameter on adsorption of Cd (II)

To study the thermodynamics of adsorption of Cd (II) on ZFA, thermodynamic constants such as enthalpy change ΔH, free energy change ΔG and entropy change ΔS were calculated using Eqs. (18)–(20). Thermodynamic parameters ΔH, ΔS and ΔG for Cd (II) ions–ZFA system were calculated using the following equations (Ahmad et al., 2009):

$$K_C = F_e/1 - F_e \tag{18}$$

$$\mathrm{Ln}K_C = \Delta S/R - \Delta H/RT \tag{19}$$

$$\Delta G = -RT\ln\ K_C \tag{20}$$

where F_e is the fraction of Cd (II) ions sorbed at equilibrium, R (8.314 J/mol K) is the gas constant, T (K) the absolute temperature and K_C (L/g) is the standard thermodynamic equilibrium constant. The enthalpy and entropy change of sorption was defined from the Ln K_C vs. $1/T$ plot (Fig. 16). The values of thermodynamic parameters are given in Table 6. A perusal of Table 6 indicated that the enthalpy change ΔH is positive (endothermic) due to an increase in adsorption on successive increase in temperature. The negative ΔG values indicated thermodynamically feasible and spontaneous nature of the sorption. The positive value of ΔS reveals the increased randomness at the solid–solution interface during the fixation of the ion on the surface of the sorbent.

3.9. Desorption experiments

After the process is done, it is vital to be able to recover the heavy metals from adsorbing agents and to reproduce and restore the used adsorbents. Batch desorption experiments were conducted and results, i.e. desorption efficiencies, were subsequently compared. Several solvents were employed for conducting the above-mentioned experiments including alkaline, acidic bases, and water. Metal-saturated adsorbents were stirred with 50 ml of solutions with a rotating speed of 200 rpm at 25 °C; desorption process was then permitted to proceed for a time period of up to 24 h. The adsorbent was then filtered and separated from solution, and dried at 100 °C. The amount of Cd (II) recovery attained using distilled water, HCl and HNO_3 with various concentrations (0.1–1 M) was not remarkable (less than 0.7% and 18% for acids and distilled water respectively). NaOH solution was then used with different concentrations (0.1–1 M). It was observed that desorption of Cd (II) from the adsorbent started at pH $\geqslant$ 8. Different concentrations of NaOH in the solution yield different regeneration percent of Cd (II)-treated ZFA ranging from 24% to 84%. Incomplete regeneration of ZFA can be due to the occurrence of some chemical reactions (for instance oxidation). As the concentration of regenerant solution (NaOH) increases, higher regeneration percentage is obtained.

To ascertain the reusability of ZFA, the adsorption–desorption cycle of Cd (II) was carried out three times with similar preparations. The obtained results are presented in Table 7. As it can be inferred from the data given in this table, the removal efficiency had not changed to a considerable amount in the process of desorption and the second and third application of ZFA has only resulted in a reduction of less than 8% in the removal efficiency.

3.10. Comparing different amounts of Cd (II) removal attained using various adsorbents reported in papers

The capacities of different adsorbents, used in this study for removal of Cd (II), were compared with those of others reported in the literature. The values presented in Table 8 were all expressed as monolayer adsorption capacity. The empirical data obtained in the present study are proportionate and comparable with those obtained in other investigations.

Table 6 Thermodynamic parameters for Cd (II) adsorption.

Cd (II)	ΔH (kj/kmol)	ΔS (kj/kmol)	ΔG (kj/mol)		
	45.615	0.172	25 °C	35 °C	45 °C
			−6.146	−7.118	−9.631

Table 7 Reusing the ZFA after desorption.

Cd (II)	Removal efficiency (%)		
	First time application of ZFA after desorption	Second time application of ZFA after desorption	Third time application of ZFA after desorption
	92.14	88.38	84.71

Table 8 Comparison of adsorption capacities of the adsorbents for the removal of Cd (II) with those of other adsorbents.

Adsorbent	q_m (mg g^{-1})	Reference
Iron ore slime	34.75	Mohapatra et al., (2009)
Syzygium cumini leaf powder	34.54	Rao et al., (2010)
Petiolar felt-sheath of palm	10.80	Iqbal et al., (2002)
Nickel laterite (high iron)	13.2	Mohapatra and Anand, (2007)
Red mud	13.03	Gupta and Sharma, (2002
Algae, Nile water	37.43	Sherif et al., (2008)
Calcite	18.52	Yavuz et al., (2007)
Perlite	0.64	Mathialagan and Viraraghavan, (2002)
Sugar beet pulp	17.20	Zacaria et al., (2002)
Manganese nodule residue	47.60	Agrawal and Sahu, (2006)
Tree fern	16.30	Ho and Wang, (2004)
Corncob	6.43	Shen and Duvnjak, (2005)
Wheat bran	0.70	Singh et al., (2006)
Rice polish	9.72	Singh et al., (2005
Exhausted coffee	1.48	Orhan and Bujukgungor, (1993)
Water hyacinth	2.44	Lu et al., (2004)
Tea-industry waste	11.29	Cay et al., (2004)
Modified lignin	6.7–7.50	Demirbas, (2004)
Nanotubes	11.00	Li et al., (2003)
Coconut copra meal	4.92	Ho and Ofomaja, (2006)
Nalco Plant Sand	58.13	Mohapatra et al., (2009)
Sawdust of Pinus sylvestris	19.09	Costodes et al., (2003)
Low grade manganese ore	59.17	(Mohapatra et al., (2008)
Fly ash, treated	14.33	Chaiyasith et al., (2006)
ZFA	26.246	Present work

4. Conclusions

It is proved that fly ash is not an appropriate adsorbent for Cd (II) removal process. Solid-state fusion reaction with NaOH creates aluminosilicate adsorbent and geopolymer with porous structures, and this way, improves the surface area, pore volume, and the capacity of adsorption for Cd (II) in aqueous solution. The optimum conditions of sorption were as follows: a sorbent dose of 0.08 g in 25 mL of Cd (II), contact time of 7 h and pH 5. The kinetic data obtained showed that pseudo-second-order equations controlled the adsorption process. Moreover, according to adsorption isotherm investigations, Langmuir equation was proved to be the best in fitting the adsorption process. Enthalpy change ΔH is positive (endothermic) due to an increase in adsorption on successive increase in temperature. The negative ΔG values indicated thermodynamically feasible and spontaneous nature of the sorption. The positive value of ΔS reveals the increased randomness at the solid solution interface during the fixation of the ion on the active sites of the sorbent. Several adsorbents, including alkaline adsorbents, bases and water were used for studying the desorption of Cd (II) from ZFA; the maximum desorption rate was obtained using 1 M of NaOH (84%). Comparative studies proved that ZFA was more efficient in removing metal ions of Cd (II) in comparison to RFA; these studies have also shown that fly ash-based geopolymer is a good alternative to more expensive adsorbents such as activated carbon in removing heavy metals from effluents and wastewaters.

References

Agrawal, A., Sahu, K.K., 2006. J. Hazard. Mater. B137, 915.
Ahmad, A., Rafatullah, M., Sulaiman, O., Ibrahim, M.H., Chii, Y.Y., Siddique, B.M., 2009. Desalination 247, 636.
Aklil, A., Mouflih, M., Sebti, S., 2004. J. Hazard. Mater. A112, 183.
Barrera-Díaz, C., Palomar-Pardavé, M., Romero-Romo, M., Ure˜na-Nu˜nez, F., 2005. J. Polym. Res. 12, 421.
Benito, Y., Ruíz, M.L., 2002. Desalination 142 (3), 229.
Boonamnuayvitaya, V., Chaiya, C., Tanthapanichakoon, W., Jarudilokkul, S., 2004. Sep. Purif. Technol. 35, 11.
Cay, S., Uyanık, A., Ozasık, A., 2004. Sep. Purif. Technol. 38, 273.
Chaiyasith, S., Chaiyasith, P., Septhum, C., 2006. Int. J. Sci. Technol. 11 (2), 13.
Chang, H.L., Chun, C.M., Aksay, I.A., Shih, W.H., 1999. Ind. Eng. Chem. Res. 38, 973.
Costodes, T.V.C., Fauduet, H., Porte, C., Delacroix, A., 2003. J. Hazard. Mater. B105, 121.
Davidovits, J., 1991. J. Therm. Anal. 37, 1633.
Dbrowski, A., Hubicki, Z., Podkocielny, P., Robens, E., 2004. Chemosphere 56 (2), 91.

Demirbas, A., 2004. J. Hazard. Mater. B109, 221.
Deng, S.B., Ting, Y.P., 2005. Langmuir 21, 5940.
Dubilin, M.M., Radushkevich, L.V., 1947. Phys. Chem. 55, 331.
El-Naggar, M.R., El-Kamash, A.M., El-Dessouky, M.I., Ghonaim, A.K., 2008a. J. Hazard. Mater. 154, 963.
El-Naggar, M.R., El-Kamash, A.M., El-Dessouky, M.I., Ghonaim, A.K., 2008b. Energy 28 (4), 535.
Ennigrou, D.J., Gzara, L., Ben Romdhane, M.R., Dhahbi, M., 2009. Desalination 246 (1-3), 363.
Fan, Y., Zhang, F.S., Feng, Y., 2008. J. Hazard. Mater. 159, 313.
Freundlich, H.M.F., 1906. Z. Phys. Chem. 57, 385.
Gerente, C., Lee, V.K.C., Le Cloirec, P., Mckay, G., 2007. Environ. Sci. Technol. 37, 41.
Ghazy, S.E., Ragab, A.H., 2007. Indian J. Chem. Technol. 14, 507.
Gonźalez, M.P.E., Mattusch, J., Wennrich, R., Morgenstern, P., 2001. Microporous Mesoporous Mater. 46, 277.
Gupta, V.K., Sharma, S., 2002. Environ. Sci. Technol. 36, 3612.
Ho, Y.S., McKay, G., 1999. Process Biochem. 34, 451.
Ho, Y.S., McKay, G., 2000. Water Res. 34, 735.
Ho, Y.S., Ofomaja, A.E., 2006. Biochem. Eng. J. 30, 117.
Ho, Y.S., Wang, C.C., 2004. Process Biochem. 39, 759.
Hui, K.S., Chao, C.Y.H., Kot, S.C., 2005. J. Hazard. Mater. B127, 89.
Iqbal, M., Saeed, A., Akhtar, N., 2002. Bioresour. Technol. 81, 151.
Jimenez, A.F., Palomo, A., 2005. Microporous Mesoporous Mater. 86, 207.
Kumar, P., Mal, N., Oumi, Y., Yamana, K., Sano, T., 2001. J. Mater. Chem. 11, 3285.
Kumar, P.A., Ray, M., Chakraborty, S., 2008. Chem. Eng. J. 141, 130.
Lagergren, S., 1898. Kung. Sven. Veten. Hand. 24, 1.
Langmuir, I., 1916. Solids. J. Am. Chem. Soc. 38 (11), 2221.
Li, Y.H., Wang, S., Luan, Z., Ding, J., Xu, C., Wu, D., 2003. Carbon 41 (5), 1057.
Lin, T.F., Wu, J.K., 2001. Water Res. 35, 2049.
Lu, X., Kruatrachue, M., Pokethitiyook, P., Homyok, K., 2004. Sci. Asia 30, 93.
Mathialagan, T., Viraraghavan, T., 2002. J. Hazard. Mater. B94, 291.
Matlock, M.M., Howerton, B.S., Atwood, D.A., 2002. Water Res. 36 (19), 4757.
McKay, G., Blair, H.S., Gardener, J.R., 1982. J. Appl. Polym. Sci. 27, 3043.
Mohammadi, T., Moheb, A., Sadrzadeh, M., Razmi, A., 2005. Sep. Purif. Technol. 41 (1), 73.
Mohan, D., Pittman, C.U., 2006. J. Hazard. Mater. 137, 762.
Mohan, D., Singh, K.P., Singh, V.K., 2005. Ind. Eng. Chem. Res. 44, 1027.
Mohan, S., Gandhimathi, R., 2009. J. Hazard. Mater. 169, 351.
Mohapatra, M., Anand, S., 2007. Indian J. Environ. Prot. 27 (6), 509.
Mohapatra, M., Khatun, S., Anand, S., 2008. Pollut. Res. 25 (3), 563.
Mohapatra, M., Rout, K., Anand, S., 2009a. J. Hazard. Mater. 171 (1–3), 417.
Mohapatra, M., Rout, K., Mohapatra, B.K., Anand, S., 2009b. J. Hazard. Mater. 166, 1506.
Molina, A., Poole, C., 2004. Miner. Eng. 17, 167.
Morris, W.J., Weber, C.I., 1963. J. San. Eng. Div. ASCE 89, 31.
Naiya, T.K., Bhattacharya, A.K., Das, S.K., 2009. Environ. Prog. Sustainable.
Naiya, T.K., Bhattacharya, A.K., Das, S.K., 2008. J. Colloid. Interface Sci. 325, 48.
Orhan, Y., Bujukgungor, H., 1993. Water Sci. Technol. 28 (2), 247.
Phair, J.W., van Deventer, J.S.J., Smith, J.D., 2004. Appl. Geochem. 19, 423.
Querol, X., Moreno, N., Umana, J.C., Alastuey, A., Hernandez, E., Lopez-Soler, A., Plana, F., 2002. Int. J. Coal Geol. 50, 413.
Rao, K.S., Anand, S., Venkateswarlu, P., 2010. Korean J. Chem. Eng.. http://dx.doi.org/10.1007/s11814-010-0243-2.
Shen, J., Duvnjak, Z., 2005. Process Biochem. 40, 3446.
Sherif, Y.E., Ashmawy, A., Badr, S., 2008. J. Appl. Sci. Res. 4 (4), 391.
Shoval, S., 2003. Opt. Mater. 24, 117.
Singh, K.K., Rastogi, R., Hasan, S.H., 2005. J. Hazard. Mater. A121, 51.
Singh, K.K., Singh, A.K., Hasan, S.H., 2006. Bioresour. Technol. 97, 994.
Tempkin, M.J., Pyzhev, V., 1940. Acta Physiochim. USSR 12, 217.
Tsang, D.C.W., Lo, I.M.C., 2006. Environ. Sci. Technol. 40, 6655.
Van Jaarsveld, J.G.S., Van Deventer, J.S.J., Schwartzman, A., 1999. Miner. Eng. 12, 75.
Voegelin, A., Kretzschmar, R., 2003. Eur. J. Soil Sci. 54, 387.
Weber, T.W., Chakraborti, R.K., 1974. J. AIChE 20, 228.
Xu, H., VanDeventer, J.S.J., 2000. Int. J. Miner. Process 59, 247.
Yavuz, O., Guzel, R., Aydin, F., Tegin, I., Ziyadanogullari, R., 2007. Polish J. Environ. Stud. 16 (3), 467.
Zacaria, R., Gerente, C., Andres, Y., Cloirec, P.L., 2002. Environ. Sci. Technol. 36, 2067.